Proton-Induced Quenching and H-D Isotope-Exchange Reactions of Methoxynaphthalenes[1]

Haruo Shizuka* and Seiji Tobita

Contribution from the Department of Chemistry, Gunma University, Kiryu, Gunma 376, Japan.
Received March 1, 1982

Abstract: Proton-induced quenching, photochemical, and thermal isotope-exchange reactions of methoxynaphthalenes in H_2O (or D_2O)–CH_3CN mixtures at moderate acid concentrations were studied by means of emission, ^1H NMR, and mass spectroscopy and measurements of reaction quantum yields. It is demonstrated that the proton-induced fluorescence quenching of 1-methoxynaphthalene (α-RH) proceeds via electrophilic protonation at the proper carbon atom of the aromatic ring in the lowest excited singlet state (^1L_a) in polar media, leading to proton exchange or isotope exchange mainly at position 5 (slightly at position 8) of the naphthalene ring. The rate constant ^1k_R for electrophilic protonation to the carbon atom of the aromatic ring in the excited state is almost equal to that of ^1k_q (the rate constant for proton-induced quenching). The isotope-exchange reaction via the triplet state is negligibly small (about 5% of that via the excited singlet state). For 2-methoxynaphthalene (β-RH) both proton-induced quenching and isotope exchange in the excited state (^1L_b) scarcely occur. The intramolecular CT structure in the excited state is responsible for the quenching. At higher temperatures ($\geq$318 K), the thermal isotope-exchange reactions of α- and β-RH take place at positions 2 and 1, respectively; the exchange rate for the latter is faster than that for the former. It is shown that the reaction rate for protonation in the excited state is extremely fast compared with that in the ground state. Activation parameters for the reactions in the excited and ground states are determined. An H–D isotope-exchange reaction mechanism is proposed on the basis of the experimental results with the aid of the usual MO calculations.

Proton association and dissociation in the excited state of aromatic compounds are elementary processes both in chemistry and biochemistry. The acid–base properties of aromatic compounds in the excited state are closely related to the corresponding electronic structure, which is considerably different from that in the ground state. Since the pioneering work of Förster[2] (1950) and Weller[3] (1952) showing that the acidity constant pK_a^* in the excited state is significantly different from that in the ground state, a number of studies on pK_a^* have been reported.[4-10] It is well-known that the pK_a^* values can be estimated by means of the Förster cycle,[2-4,11] the fluorescence titration curves,[3,4] and the $T_n \leftarrow T_1$ absorbance titration curve.[12] These methods involve the assumptions that proton transfer in the excited state is very fast and the acid–base equilibrium may be attained during the lifetime of the excited state. A laser study of the protonation equilibrium of triplet benzophenone has been reported by Rayner and Wyatt.[13] Similar equilibria in the triplet state of other aromatic ketones have been recently demonstrated, since the triplet lifetime is long enough to allow the acid–base equilibrium.[14]

However, it has been shown by Tsutsumi and Shizuka[15] (1977) the proton-induced fluorescence quenching competitive with proton transfer reactions is present in the excited state of neutral naphthylamines (that is, the simple acid–base equilibrium cannot be accomplished in the excited state of aromatic amines) and the dynamic analyses containing the proton-induced quenching are, therefore, needed in order to obtain the correct pK_a^* values. The dynamic analyses by means of nanosecond time-resolved spectroscopy with fluorimetry were applied to 1-aminopyrene,[16] 1-aminoanthracene,[17] phenanthrylamines,[18] and naphthols.[19] Recently, the Stuttgart group[20] has supported our method to determine the pK_a^* values of naphthylamines. Similar experiments for excited naphthols have been reported by Harris and Selinger.[21] Establishment of prototropic equilibrium in the excited singlet state at moderate acid concentrations has been reported in the cases of 2-naphthol-6,8-disulfonate[22] and 2-naphthol.[19]

For the proton-induced quenching mechanism, a complex in which a proton is shared between excited 2-naphthalamine and one water molecule[23] or a hydrated naphthylammonium cation in the ground state[24] was assumed as an intermediate for the quenching. However, little attention to the quenching mechanism has yet been given. In preliminary accounts,[1] it has been reported that the proton-induced quenching at moderate acid concentrations $[H_2SO_4] \leq 0.1$ M is caused by electrophilic protonation at one of the carbon atoms of the aromatic ring in the excited state leading to proton exchange (or isotope exchange).

Since the original work of Havinga[25] (1956) on isotope exchange in the excited state of aromatic compounds, several studies on the subject have been reported.[26-30] For naphthalene, Stevens and

(1) Preliminary accounts of the present paper: Tobita, S.; Shizuka, H. presented in part at the VIII IUPAC Symposium on Photochemistry at Seefeld, Austria, July, 1980; *Chem. Phys. Lett.* **1980**, *75*, 140. This work was supported by Scientific Research Grant-in-Aid of the Ministry of Education of Japan (No. 410404).
(2) Förster, Th. *Z. Elektrochem. Angew. Phys. Chem.* **1950**, *54*, 42, 531.
(3) Weller, A. *Ber. Bunsenges, Phys. Chem.* **1952**, *56*, 662; **1956**, *66*, 1144.
(4) Weller, A. *Prog. React. Kinet.* **1970**, *5*, 273.
(5) Beens, H.; Grellman, K. H.; Gurr, M.; Weller, A. *Discuss. Faraday Soc.* **1965**, *39*, 183.
(6) Donckt, E. V. *Prog. React. Kinet.* **1970**, *5*, 273.
(7) Ireland, J. F.; Wyatt, P. A. H. *Adv. Phys. Org. Chem.* **1976**, *12*, 131, and a number of references therein.
(8) Wehry E. L.; Rogers, L. B. In "Fluorescence and Phosphorescence Analyses"; Hercules, D. M., Ed.; Wiley-Interscience: New York, 1966, p 125.
(9) Klöpffer, W. *Adv. Photochem.*, **1977**, *10*, 311.
(10) Schulman, S. G. In "Modern Fluorescence Spectroscopy", Vol. 2, Wehry, E. L., Ed.; Plenum: New York, 1976.
(11) Grabowski, Z. R.; Grabowska, A. *Z. Phys. Chem. (Wiesbaden)* **1976**, *101*, 197.
(12) Jackson, G.; Porter, G. *Proc. R. Soc. London, Ser. A*, **1961**, *200*, 13.
(13) Rayner, D. M.; Wyatt, P. A. H. *J. Chem. Soc., Faraday Trans. 2*, **1974**, *70*, 945.
(14) Shizuka, H.; Takada, K. presented at Symposium on Molecular Structures, Kyoto, Oct 1981.
(15) (a) Tsutsumi, K.; Shizuka, H. *Chem. Phys. Lett.* **1977**, *52*, 485; (b) *Z. Phys. Chem. (Wiesbaden)*, **1978**, *111*, 129.
(16) Shizuka, H.; Tsutsumi, K.; Takeuchi, H.; Tanaka, I. *Chem. Phys. Lett.* **1979**, *62*, 408; *Chem. Phys.* **1981**, *59*, 183. Proton-transfer reactions in the excited state have also been studied by means of picosecond spectroscopy.
(17) Shizuka, H.; Tsutsumi, K. *J. Photochem.* **1978**, *9*, 334.
(18) Tsutsumi, K.; Sekiguchi, S.; Shizuka, H. *J. Chem. Soc., Faraday Trans. 1* **1982**, *78*, 1087.
(19) Tsutsumi, K.; Shizuka, H. *Z. Phys. Chem. (Wiesbaden)* **1980**, *122*, 129.
(20) Hafner, F.; Wörner, J.; Steiner, U.; Hauser, M. *Chem. Phys. Lett.* **1980**, *72*, 139.
(21) Harris, C. M.; Selinger, B. K. *J. Phys. Chem.* **1980**, *84*, 891, 1366.
(22) Schulman, S. G.; Rosenberg, L. S.; Vincent, Jr., W. R. *J. Am. Chem. Soc.* **1979**, *101*, 139.
(23) Förster, Th. *Chem. Phys. Lett.* **1972**, *17*, 309.
(24) Schulman, S. G.; Sturgeon, R. J. *J. Am. Chem. Soc.* **1977**, *99*, 7209.
(25) (a) Havinga, E.; de Jongh, R. O.; Dorst, W. *Recl. Trav. Chim. Pays-Bas*, **1956**, *75*, 378. (b) Havinga, E.; Kronenberg, M. E. *Pure Appl. Chem.* **1968**, *16*, 137. (c) de Bie, D. A.; Havinga, E. *Tetrahedron* **1965**, *21*, 2395. (d) Lodder, G.; Havinga, E. *Ibid.* **1972**, *28*, 5583.
(26) Stevens, C. G.; Strickler, S. J. *J. Am. Chem. Soc.* **1973**, *95*, 3922.
(27) Colpa, J. P.; Maclean, C.; Mackor, E. L. *Tetrahedron, Suppl.* **1963**, *2*, 65.
(28) Kuz'min, M. G.; Uehinov, B. M.; Szent Gyorgy, G.; Berezin, I. V. *Russ. J. Phys. Chem.* **1967**, *41*, 400.
(29) Vesley, G. F. *J. Phys. Chem.* **1971**, *75*, 1775.

0002-7863/82/1504-6919$01.25/0

Strickler[26] reported the H–D isotope exchange and fluorescence quenching at higher acid concentrations (% H_2SO_4 = 30–77). The demonstration of fluorescence quenching by acids suggests that the lowest excited singlet state is involved in prototropic reactions.[26-28] However, the reactive state for isotope exchange in excited anthracene was assumed to be the triplet state.[28] Vesley[29] considered that both singlet and triplet states are involved in the photochemical isotope-exchange reactions in *p*-hydroquinone. Similarly, from comparison of the observed substitution pattern of toluene with excited-state electron distributions involvement of the second excited singlet and the lowest triplet states as the reactive states was pointed out by Spillane.[30] These isotope-exchange reactions in the excited state give rise to a significant enhancement of the reaction rates and also changes in the relative positional reactivities compared to those in the ground state. However, the isotope-exchange mechanism in the excited state has not yet been established.

On the other hand, quantum mechanical theories have been successful in elucidation or prediction of chemical reactions.[31-35] The original examples for the reactive indices are the charge density by Coulson and Longuet-Higgins,[36] the free valence number by Coulson,[37] the frontier electron density[38a] and super delocalizability[38b] by Fukui, and localization energies by Wheland.[39] It was expected that the reactive indices for electrophilic reactions obtained by the usual MO methods (except for the free valence number) might interpret the isotope-exchange reactions both in the excited and ground states, since they were considered to be typical electrophilic reactions.

In a course of a study on proton-transfer reactions in the excited state, we became interested in photochemical and thermal isotope-exchange reactions of aromatic compounds from the following viewpoints: (1) What is the proton-induced quenching mechanism? (2) Is there any relation between the proton-induced quenching and the photochemical isotope-exchange reaction? (3) Is there any difference in chemical reactivities (reactive positions and rates) for the electrophilic H–D isotope exchange reactions between the excited and ground states? (4) What about the potential energy state diagram for the photochemical and thermal isotope-exchange reactions? Methoxynaphthalenes were chosen as model compounds for the isotope-exchange reactions since the compounds were photochemically stable compared with those of naphthylamines.[15b] In the present paper, the proton-induced quenching in H_2O (or D_2O)–CH_3CN mixtures has been further investigated by means of nanosecond time-resolved spectroscopy with fluorimetry, and the photochemical and thermal H–D isotope exchange reactions have also been studied by means of ^1H NMR and mass spectroscopy and measurements of the reaction quantum yields with the aid of the usual MO methods (semiempirical SCF MO CI and extended Hückel MO methods).

Experimental Section

Materials. Aromatic compounds (G. R. grade products from Tokyo Kasei) were purified by repeated recrystallizations. For liquid samples (Tokyo Kasei), they were purified by passing each reagent through a silica gel column using benzene as a developing solvent. H_2SO_4 (97%, Junsei), D_2O (99.5%), Merck), and D_2SO_4 (96–98%, isotope purity 99%, Merck) were used without further purification. Deionized water was distilled. Acetonitrile (reagent grade) was purified by the usual method.[40] The actual acid contents were determined by titration.

Proton-Induced Fluorescence Quenching. The concentrations of the samples for proton-induced quenching were 10^{-4} to 10^{-5} M in H_2O (or D_2O)–acetonitrile (4:1 or 1:4 in volume) mixtures. All samples were thoroughly degassed by freeze–pump–thaw cycles on a high-vacuum line.[41] Fluorescence intensities were recorded with a Hitachi MPF 2A fluorimeter and the spectral corrections due to the apparatus were made. The fluorescence quantum yields were measured by comparison with a quinine bisulfate 0.1 N H_2SO_4 solution (Φ_F = 0.54).[42,43] Fluorescence lifetimes were measured by a Hitachi nanosecond time-resolved fluorimeter (pulse width 11 ns), and the convolution method was applied when they were shorter than 20 ns. The fluorescence polarization measurements were carried out in glycerol using a cryostat (Oxford DN704) at lower temperatures ≤260 K. In order to check the triplet–triplet energy transfer from benzophenone to 1-methoxynaphthalene, we employed a Q-switched ruby laser (JEOL, JLS-R3A, half-width 23ns) at 347 nm.[44]

Photochemical and Thermal Isotope-Exchange Reactions. The photochemical isotope-exchange reactions were carried out with 5×10^{-3} M 1- (or 2-) methoxynaphthalene in a D_2O–CH_3CN (1:4) mixture with $[D_2SO_4]$ = 0.05 M. A low-pressure mercury lamp with a Vycor glass filter was used as the 254-nm radiation source, while a medium-pressure mercury lamp with an interference glass filter was used as the 366-nm source. Actinometry was carried out with a ferric oxalate solution.[45] After a definite time of irradiation, the sample solutions were extracted with benzene, followed by evaporation under reduced pressure. The resulting residue consisting of methoxynaphthalene with small amounts of photochemical products (<10%) was purified by passing it through a silica gel column with benzene as a developing solvent.

The thermal isotope-exchange reactions were performed with a 1×10^{-2} M 1- (or 2-) methoxynaphthalene D_2O–CH_3CN (1:4) mixed solution with $[D_2SO_4]$ = 0.05 M. The treatments of the sample solutions were the same as those in the case of photochemical reactions.

The H–D isotope-exchange positions of methoxynaphthalenes were determined by means of ^1H NMR spectroscopy (JEOL PS 100), and quantitative analyses for isotope exchange were carried out by means of mass spectroscopy (Hitachi RMU-7M). In order to avoid ion fragmentation, the electron accelerating voltage was reduced to 10 eV. The relative peak height was corrected for the contribution from naturally abundant ^{13}C of methoxynaphthalenes (12.3%).

Methods of Calculations

Semiempirical SCF MO CI Method. The electronic structures of methoxynaphthalenes were studied by the variable β,γ procedure of the semiempirical SCF MO method combined with a singly excited CI calculation. The parameters were taken as proposed by Nishimoto and Forster.[46] The one-center electron repulsion integrals $\gamma_{\mu\mu}$ were estimated from the corresponding valence-state ionization potentials (I_μ) and electron affinities (A_μ) by the Pariser–Parr approximation,[47] I_μ and A_μ being determined from spectroscopic data using the promotion energies of Hinze and Jaffé.[48] The two-center electron repulsion integrals $\gamma_{\mu\nu}$ were estimated by the use of the Nishimoto–Mataga approximation.[49] The two-center core resonance integrals $\beta_{\mu\nu}$ were evaluated by the Nishimoto–Forster approximation.[46] The C–C and C–O bond lengths were assumed to be 1.39 and 1.36 Å, respectively. All bond angles were assumed to be 120°.

(30) Spillane, W. J. *Tetrahedron*, **1975**, *31*, 495.
(31) Streitwieser, Jr., A. "Molecular Orbital Theory for Organic Chemists"; Wiley: New York, 1961.
(32) Salem, L. "The Molecular Orbital Theory of Conjugated Systems"; Benjamin: New York, 1966.
(33) Dewar, M. J. S. "The Molecular Orbital Theory of Organic Chemistry"; McGraw-Hill: New York, 1969.
(34) Woodward, R. B.; Hoffmann, R. "The Conservation of Orbital Symmetry"; Verlag-Chemie: Weinheim, 1970.
(35) Fleming, I. "Frontier Orbitals and Organic Chemical Reactions"; Wiley-Interscience: New York, 1976.
(36) Coulson, C. A.; Longuet-Higgins, H. C. *Proc. R. Soc. London, Ser. A* **1947**, *191*, 39.
(37) Coulson, C. A. *Dicuss. Faraday Soc.* **1947**, *2*, 9.
(38) (a) Fukui, K.; Yonezawa, T.; Shingu, H. *J. Chem. Phys.* **1952**, *20*, 722. (b) Fukui, K.; Yonezawa, T.; Nagata, C. *Bull. Chem. Soc. Jpn.* **1954**, *27*, 423.
(39) Wheland, G. W. *J. Am. Chem. Soc.* **1942**, *64*, 900.
(40) Weissberger, A.; Proskauer, E. S.; Riddick, J. A.; Troops, Jr., E. E. "Organic Solvents"; Wiley-Interscience: New York, 1955, p 435.
(41) For 1-methoxynaphthalene in aerated H_2O–CH_3CN mixtures with protons, the photochemical reactions took place appreciably to yield red products at 254 nm and 300 K.
(42) Melhuish, M. H. *J. Phys. Chem.* **1961**, *65*, 229.
(43) Damas, J. N.; Crosby, G. A. *J. Phys. Chem.* **1971**, *75*, 991.
(44) Details for the apparatus and procedures have been described elsewhere: e.g., Shizuka, H.; Nakamura, M.; Morita, T. *J. Phys. Chem.* **1980**, *84*, 989.
(45) Hatchard, C. G.; Parker, C. A. *Proc. R. Soc. London, Ser. A*, **1956**, *235*, 518. For details, see the following reference: de Mayo, P.; Shizuka, H. In "Creation and Detection of the Excited State", Ware, W. R. Ed.; Marcel Dekker: New York, Vol. 4, Chapter 4.
(46) Nishimoto, K.; Forster, L. S.; *Theoret. Chim. Acta*, **1965**, *3*, 407; **1966**, *4*, 155.
(47) Pariser, R.; Parr, R. G. *J. Chem. Phys.* **1953**, *21*, 446, 767; Parr, R. G. "Quantum Theory of Molecular Electronic Structure"; Benjamin: New York, 1964.
(48) Hinze, J.; Jaffé, H. H. *J. Am. Chem. Soc.* **1962**, *84*, 540.
(49) Nishimoto, K.; Mataga, N. *Z. Phys. Chem. (Wiesbaden)* **1957**, *12*, 335; **1957**, *13*, 140.

Table I. Stern-Volmer Constants (K_{SV}), Fluorescence Lifetimes (τ^0) and Quantum Yields ($\Phi_f{}^0$) without Acids, Quenching Rate Constants (^1k_q), and Ionization Potentials ($I_P{}^*$) in the Excited State of Aromatic Compounds at 300 K[a]

sample	solvent	quencher	K_{SV}/M^{-1}	τ_0/ns	$\Phi_f{}^0$	$^1k_q/10^9$ M^{-1} s^{-1}	$E_A{}^*$[b]/ eV	$I_P{}^*$[c]/ eV
1-methoxynaphthalene	20% CH_3CN in H_2O	H^+	9.6	8.9	0.43	1.08	3.87	3.91
	20% CH_3CN in D_2O	D^+	4.8	9.4	0.41	0.51		
	80% CH_3CN in H_2O	H^+	2.2	12.6	0.36	0.16		
	80% CH_3CN in D_2O	D^+	1.1	12.8	0.42	9.0×10^{-2}		
2-methoxynaphthalene	20% CH_3CN in H_2O	H^+	<0.03	10	0.33	$<3 \times 10^{-3}$	3.68	4.24
1-cyanonaphthalene	20% CH_3CN in H_2O	H^+	0.28	4.4	0.37	6.4×10^{-2}	3.87	5.43[d]
2-cyanonaphthalene	20% CH_3CN in H_2O	H^+	0.29	12	0.53	2.4×10^{-2}		
1-naphthylamine[e]	5% CH_3CN in H_2O	H^+	2.4×10^2	27	0.49	8.9	3.24	4.06
	5% CH_3CN in D_2O	D^+	$1.7_4 \times 10^2$	29	0.56	6.0		
2-naphthylamine[e]	5% CH_3CN in H_2O	H^+	6.3	19	0.45	0.33	3.32	3.93
	5% CH_3CN in D_2O	D^+	3.19	20	0.47	0.19_6		
1-naphthol[f]	H_2O	H^+	[g]	7.8[h]	1.3×10^{-3} [h]	0.75[g]	3.57	4.13[d]
	D_2O	D^+	[g]	9.0[h]	2.1×10^{-3} [h]	0.46[g]		
2-naphthol[f]	H_2O	H^+	[g]	7.9[h]	0.21_4[h]	<0.03[g]	3.64	4.18[d]
	D_2O	D^+	[g]	8.6[h]	0.23[h]	<0.02[g]		
naphthalene	20% EtOH in H_2O	H^+	$<4.3 \times 10^{-2}$	43		$<1 \times 10^{-3}$	3.98	4.20
1-aminoanthracene[i]	20% CH_3CN in H_2O	H^+	[g]	4.1	5.1×10^{-3}	0.12[g]	2.64	4.3[d]
	20% CH_3CN in D_2O	D^+	[g]	20	7.8×10^{-2}	0.02[g]		
anthracene[j]	MeOH	H_2SO_4	$<3.8 \times 10^{-2}$	3.8		$<1 \times 10^{-2}$	3.31	4.24
9,9′-bianthryl[j]	MeOH	H_2SO_4	57	37	0.21	1.54		
1-aminopyrene[k]	50% CH_3CN in H_2O	H^+	7×10^{-2}	5.4	0.54	1.3×10^{-2}	3.02	3.91[d]
	50% CH_3CN in D_2O	D^+	5.4×10^{-2}	8.0	0.61	0.68×10^{-2}		
pyrene	30% MeOH in H_2O	H^+	$<3.5 \times 10^{-2}$	3.5×10^2		$<1 \times 10^{-4}$	3.33	4.22

[a] Experimental errors within ±5%. [b] $E_A{}^*$ denotes the 0-0 transition energy for $^1A^*$-^1A. [c] $I_P{}^* = I_P - E_A{}^*$. The $I_P{}^*$ value is regarded as a measure of the tendency of electron donating power of $^1A^*$, although it may involve a deviation from the real value. [d] The value of I_P was estimated by the usual CT method using tetracyanoethylene. [e] Data taken from ref 15. [f] Data taken from ref 19. [g] Determined by the dynamic analyses. [h] $[H^+]$ (or $[D^+]$) = 0.1 N in H_2O or D_2O at 300 K. [i] Data taken from ref 17. [j] Data taken from ref 53. [k] Data taken from ref 16.

Extended Hückel MO Method. The extended-Hückel MO method is a well-established procedure for all valence-electron systems as has been originally developed by Hoffmann.[50] The diagonal matrix elements H_{ff} were estimated from the corresponding valence-state ionization potentials as reported by Skinner and Pritchard.[51] The off-diagonal matrix elements H_{fj} were approximated by the Wolfsberg and Helmholtz method.[52] The calculations were carried out using a HITAC 8800/8700 located at the Computer Center of the University of Tokyo.

Results and Discussion

Proton-Induced Fluorescence Quenching. Proton-induced fluorescence quenching of aromatic compounds has been studied in polar solvents at moderate acid concentrations ($[H_2SO_4] \leq 0.3$ M). Excited aromatic molecules $^1A^*$ having an intramolecular charge-transfer structure in the fluorescent state (e.g., 1-methoxynaphthalene, 1-naphthol,[19] naphthylamines,[15] phenanthrylamines,[18] 1-aminoanthracene,[17] 1-aminopyrene,[16] and 9,9′-bianthryl)[53] were quenched effectively by protons. However, the quenching for aromatic compounds having no (or very weak) intramolecular CT character in the fluorescent state such as naphthalene, 2-methoxynaphthalene, anthracene, and pyrene was scarcely observed.

For example, the fluorescence quenching of 1-methoxynaphthalene (α-RH) by protons occurred significantly without any change in shape of absorption and fluorescence spectra as shown in Figure 1. No quenching effect due to the counteranion $SO_4{}^{2-}$ was observed under the experimental conditions. The Stern–Volmer plot of $I_f{}^0/I_f$ (or τ_0/τ) vs. $[H_3O^+]$ gave a linear relation (Figure 2). Here I_f and $I_f{}^0$ denote relative fluorescence intensities and τ and τ_0[54] fluorescence lifetimes with and without

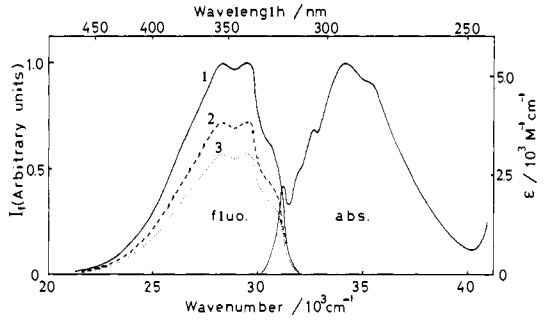

Figure 1. Absorption and fluorescence spectra of a 1.4×10^{-4} M H_2O–CH_3CN (4:1) solution of α-RH with and without H_2SO_4: (1) blank; (2) $[H_2SO_4]$ = 0.02 M; (3) $[H_2SO_4]$ = 0.04 M.

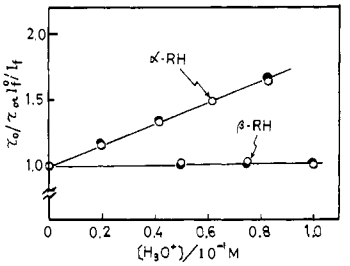

Figure 2. The Stern–Volmer plot of τ_0/τ (or $I_f{}^0/I_f$) as a function of $[H_3O^+]$ for α- and β-RH in H_2O–CH_3CN (4:1) mixtures at 300 K: (○) τ_0/τ; (●) $I_f{}^0/I_f$.

protons, respectively. The quenching rate constants ^1k_q can be determined from eq 1.

$$\frac{I_f^0}{I_f}\left(=\frac{\tau_0}{\tau}\right) = 1 + {}^1k_q\tau_0[H_3O^+] \qquad (1)$$

The ^1k_q values obtained are listed in Table I. For 2-methoxynaphthalene (β-RH) the quenching was not appreciable in the measurements of τ and I_f at the fluorescence maximum (28.8×10^3 cm^{-1}). The Stern–Volmer plot for β-RH is shown in Figure 2. The quenching results of methoxynaphthalenes are very similar

(50) Hoffmann, R. *J. Chem. Phys.* **1963**, *39*, 1397.
(51) Skinner, H. A.; Pritchard, H. O. *Trans. Faraday Soc.* **1953**, *49*, 1254.
(52) Wolfsberg, M.; Helmholtz, L. *J. Chem. Phys.* **1952**, *20*, 837.
(53) Shizuka, H.; Ishii, Y.; Morita, T. *Chem. Phys. Lett.* **1979**, *62*, 408.
(54) The fluorescence response functions of α-RH were measured at the fluorescence maxima 29.8×10^3 cm^{-1} (3.69 eV) and 27.9×10^3 cm^{-1} (3.46 eV) corresponding to the emissions $^1L_b \rightarrow {}^1A$ and $^1L_a \rightarrow {}^1A$, respectively. However, there was no appreciable difference in the decay functions between them indicating that a fast equilibrium between ^1L_b and ^1L_a might be established in the fluorescent state at room temperature.

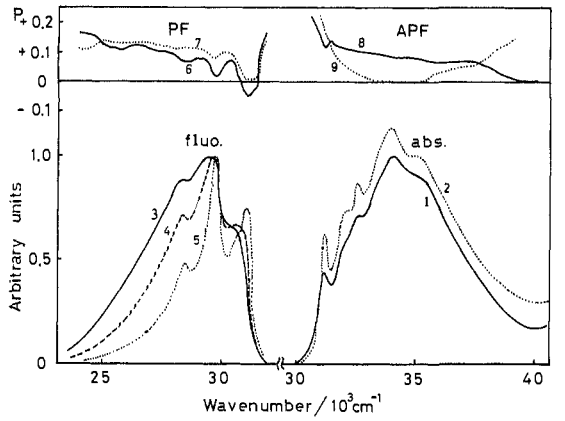

Figure 3. The absorption, fluorescence, and polarization spectra of α-RH in glycerol. Absorption spectra (abs.): (1) at 300 K; (2) at 200 K. Fluorescence spectra (fluo.) excited at 33.9×10^3 cm^{-1}: (3) at 323 K; (4) at 260 K; (5) at 200 K. Fluorescence polarization spectra (PF) excited at 33.9×10^3 cm^{-1}: (6) at 200 K; (7) at 283 K. Fluorescence excitation polarization spectra (APF): (8) observed at 200 K and 27.8×10^3 cm^{-1}; (9) observed at 200 K and 30.8×10^3 cm^{-1}. The degree of polarization (P) is given by $P = (I_\parallel - I_\perp)(I_\parallel + I_\perp)^{-1}$; Albrecht, A. C. *J. Mol. Spectrosc.* **1961**, *6*, 84.

to those of naphthols; the proton-induced quenching of 1-naphthol takes place effectively but not appreciably for 2-naphthol.[19] It was confirmed from the fluorescence polarization experiments in glycerol that the fluorescent state of α-RH has an intramolecular CT structure (^1L_a) in contrast to the (^1L_b) of β-RH. Figure 3 shows the absorption, fluorescence, and polarization spectra of α-RH in glycerol at several temperatures. The fluorescence of α-RH at longer wavelengths (358 nm) at higher temperatures (≥260 K) originates from an intramolecular CT state (^1L_a) resulting from inversion of the electronic levels (^1L_b and ^1L_a) of α-RH during the lifetime of the excited state in a solvent-assisted relaxation process. Similar features for 1- and 2-naphthols have been studied by Suzuki et al.[55] The value of ^1k_q in the H_2O (or D_2O)–CH_3CN (4:1) system is greater than that in the H_2O (or D_2O)–CH_3CN (1:4). This is due to relatively small CT character (^1L_a) in the fluorescent state even at 300 K in addition to a decrease in the activity of acid in the latter solvent system. A high water content of a mixed solvent is, consequently, favorable to the proton-induced quenching (Table I).

It is noteworthy that there is relatively little correlation between ^1k_q and I_p^* [the ionization potential for $^1A^*$ estimated from I_p (ionization potential for the ground state ^1A) minus E_A^* (0–0 transition energy for $^1A^*$–^1A)]. The quenching mechanism of $^1A^*$ by protons is, therefore, different from that by inorganic anions $^1X^-$.[44,56] The former involves a chemical interaction (protonation) at one of the carbon atoms of the aromatic ring as is shown later, and the latter involves an electron-transfer (or charge-transfer) process. An electronic interaction between $^1A^*$ and H^+ (or D^+) in the quenching is locally restricted to one of the carbon atoms of the aromatic nucleus. This phenomenon may be attributed to the following reasons: the radius of the proton (10^{-5} Å)[57] is too small to overlap widely with the π-electron system of $^1A^*$ compared with those of $^1X^-$ (1.5–3 Å), and electrostatic and covalent interactions between H^+ (or D^+) and the proper carbon atom of $^1A^*$ become large enough to give bond formation (i.e., protonation).

The introduction of electron donating groups such as amino, hydroxy, and methoxy groups into the aromatic ring causes electron migration from the substituents to the ring in the excited state. This tendency is enhanced by solvation of $^1A^*$ in polar media as described above. Thus, $^1A^*$ has an intramolecular CT structure. As a result, the basicity of the aromatic ring increases appreciably in the excited state. This is the reason why the intramolecular CT structure is responsible for the proton-induced quenching. The CT character in $^1A^*$ having electron-donating moieties at the α-position of the naphthalene ring is larger than that at the β-position. Therefore, the values of ^1k_q for the former become greater than for the latter as shown in Table I.

For an electron-withdrawing group such as the cyano group, the reverse electron migration from the aromatic ring into the substituent may contribute to the fluorescence quenching by protons: that is, the quenching may be caused by an interaction between the substituent and protons.

There are considerable kinetic isotope effects on proton-induced quenching: the ^1k_q values in the H^+ quencher system are greater than those in the D^+ system as shown in Table I.

Photochemical and Thermal Isotope-Exchange Reactions. The H–D isotope-exchange reactions both in the ground and excited states of methoxynaphthalenes (RH) as model compounds have been carried out to clarify the proton-induced quenching mechanism of aromatic compounds. The photochemical isotope-exchange reaction was performed in a 5×10^{-3} M D_2O–CH_3CN (1:4) solution of α-RH with $[D_2SO_4] = 0.05$ M at 300 K. Figure 4 shows 100-MHz ^1H NMR spectra of α-RH in CCl_4 (a) before irradiation and (b) after irradiation for 10 h at 254 nm and 300 K. As expected from the quenching results (Table I), for α-RH the isotope-exchange reaction took place markedly upon irradiation at 254 nm, but not appreciably for β-RH for 50 h at 254 nm and

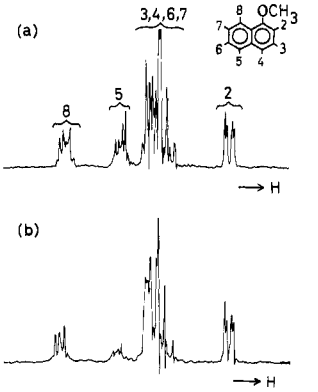

Figure 4. The 100-MHz ^1H NMR spectra of α-RH in CCl_4: (a) before irradiation; (b) after irradiation for 10 h at 254 nm and 300 K in a D_2O–CH_3CN (1:4) mixture with $[D_2SO_4] = 0.05$ M. The 100-MHz ^1H NMR spectra of RH were assigned from the data reported by Lucchini and Wells: Lucchini, V.; Wells, R. P. *Org. Magn. Reson.* **1976**, *8*, 137.

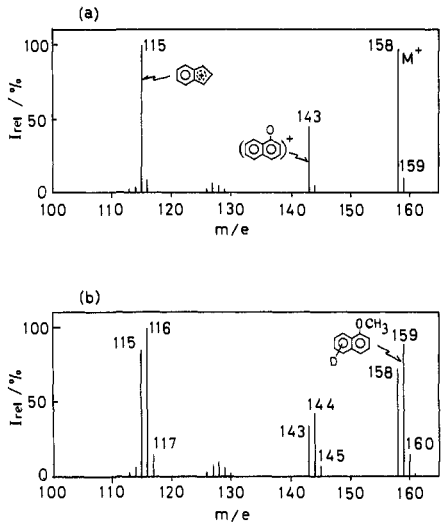

Figure 5. Mass spectra of α-RH: (a) before irradiation and (b) after irradiation for 10 h at 254 nm and 300 K in a D_2O–CH_3CN (1:4) mixture with $[D_2SO_4] = 0.05$ M.

(55) Suzuki, S.; Fujii, T.; Sato, K. *Bull. Chem. Soc. Jpn.* **1972**, *45*, 1937; Suzuki, H.; Baba, H. *Ibid.* **1967**, *40*, 2199.
(56) Shizuka, H.; Obuchi, H. *J. Phys. Chem.* **1982**, *86*, 1297.
(57) Protons exist in water as hydronium ions. However, protonation proceeds via proton transfer involving only the movement of a nucleus as has been stated by Bell: Bell, R. P. "The Proton in Chemistry"; Chapman and Hall: London, 1973.

Table II. Photochemical and Thermal Isotope-Exchange Reactions of Methoxynaphthalenes in D_2O–CH_3CN (1:4) Mixtures at Moderate Acid Concentrations at 300 K[a]

sample		$[D_3O^+]$/ M	reaction temp/ K	reaction time/ h	deuterium content/% D-1	D-2	D-3	D-4	D-5	D-6	D-7	D-8	recovery/ %
α-RH	$h\nu$[b]	0.05	300	10	0				45			5	90
	Δ	0.1	348	30	0	21							97–98
	δ/ppm[c]				0	6.64	7.23	7.29	7.66	7.36	7.35	8.17	
β-RH	$h\nu$[b,d]	0.05	300	50		0							
	Δ	0.1	348	10	18	0							97–98
	δ/ppm[c]				6.97	0	7.04	7.60	7.64	7.21	7.32	7.60	

[a] The concentrations of the starting materials were 5×10^{-3} M and 1×10^{-2} M for photochemical and thermal reactions, respectively. [b] Excitation at 254 nm. [c] The 100-MHz ^1H NMR data of methoxynaphthalenes were taken from the data reported by Lucchini and Wells: Lucchini, V; Wells, P. R. *Org. Magn. Reson.* 1976, *8*, 137. [d] The quantum yield for isotope exchange of β-RH at 254 nm was less than 1×10^{-3} at $[D_3O^+] = 0.1$ M at 300 K.

Table III. Singlet and Triplet Quenching Yields ($^1\Phi_q$; $^3\Phi_q$, Respectively) and Reaction Quantum Yields ($^1\Phi_R$; $^3\Phi_R$, Respectively) at $[D_3O^+] = 0.1$ M and 300 K

sample	solvent D_2O: CH_3CN	$^1\Phi_q$[b]	$^3\Phi_q$[c]	$^1\Phi_R$	$^3\Phi_R$[c]
α-RH	1:4	0.10_2	<0.01	0.05	0.004
	4:1	0.32_4		0.24	
β-RH	1:4	$<2 \times 10^{-3}$		$<2 \times 10^{-3}$	

[a] Experimental errors ±10%. [b] $^1\Phi_q = {}^1k_q\tau[D_3O^+]$. [c] Sensitized by triplet benzophenone at 366 nm.

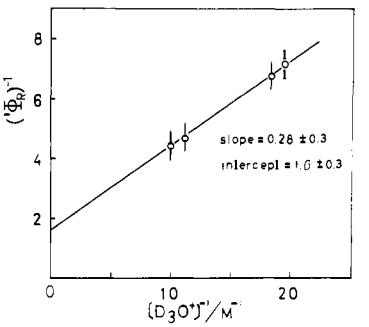

Figure 6. Plot of $(^1\Phi_R)^{-1}$ vs. $[D_3O^+]^{-1}$, where $^1\Phi_R$ denotes the reaction quantum yield for isotope exchange in D_2O–CH_3CN (4:1) mixtures at 254 nm and 300 K.

300 K. The exchange positions in the excited state of α-RH were assigned to be mainly position 5, and slightly position 8, of the naphthalene ring by means of ^1H NMR and MS methods. Figure 5 shows mass spectra of α-RH: (a) before irradiation and (b) after irradiation for 10 h at 254 nm and 300 K. The results of photochemical isotope-exchange reactions of RH are shown in Table II. Under the experimental conditions at moderate acid concentrations ($[D_3O^+] \leq 0.1$ M) and 300 K, there was no appreciable isotope exchange in the ground state of RH. Other photochemical reactions[41] were very small under the experimental conditions judging from the high recovery of the starting materials as shown in Table II.

At higher temperatures (e.g., 348 K), thermal isotope-exchange reactions occurred both in α- and β-RH: the exchange positions were position 2 for the α-isomer and position 1 for the β-isomer. In contrast to the photochemical reactions, the exchange rate of β-RH is faster than that for α-RH in the ground state. The exchange positions in the ground state are quite different from those in the excited state.

Reaction Scheme for Proton-Induced Quenching. Quantitative measurements of the photochemical H–D isotope exchange reactions have been carried out. For example, the quantum yields for isotope exchange in the excited state of α-RH were 0.24 (±0.2) in a D_2O–CH_3CN (4:1) mixture and 0.05 in D_2O–CH_3CN (1:4) mixture at $[D_3O^+] = 0.1$ M at 254 nm and 300 K. From measurements of the triplet sensitization of α-RH by benzophenone at 366 nm,[58] it was found that the quantum yield for isotope exchange in the triplet state of α-RH is about 10% relative to that in the excited singlet state. That is, for direct excitation at 254 nm, the quantum yield via the triplet state is evaluated to be ~5% of that via the excited singlet state at $[D_3O^+] = 0.1$ M. The quantum yields for isotope exchange as well as those for singlet and triplet quenching at $[D_3O^+] = 0.1$ M are listed in Table III. These data give additional examples[28,56,59] that for ionic interactions

Scheme I

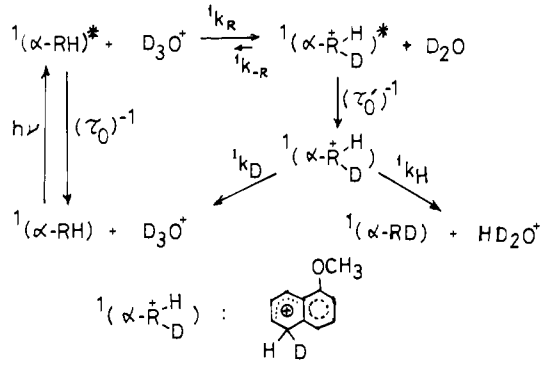

the excited singlet state is very much superior to the triplet state considering their electronic structures (ionic- and radical-like structures, respectively). It is reasonable to conclude that the H–D isotope exchange reactions in the excited singlet state originates from the lowest excited singlet state (^1L_a) of α-RH in polar media. The experimental results can be accounted for by Scheme I, as is discussed later in details, where $^1(\alpha\text{-RH})^*$ denotes the lowest excited singlet state (^1L_a) of α-RH, $^1(\alpha\text{-}^+\text{RHD})$ and $^1(\alpha\text{-}^+\text{RHD})^*$ are the σ-complex deuterated at position 5 of α-RH in the ground and excited states, respectively, ^1k_R and $^1k_{-R}$ are the rate constants for the D^+ association and dissociation processes, respectively, ^1k_H and ^1k_D are the rate constants for H^+ and D^+ dissociation processes from $^1(\alpha\text{-}^+\text{RHD})$, respectively, and τ_0' is the lifetime of $^1(\alpha\text{-}^1\text{RHD})^*$. This mechanism supports Weller's prediction quoted in ref 23 that naphthylamine in the excited singlet state should be very susceptible to electrophilic attack at one of the aromatic carbon atoms.

From the steady-state approximation, the quantum yield for isotope exchange $^1\Phi_R$ is given by

$$^1\Phi_R = \frac{^1k_H}{^1k_H + {}^1k_D} \times \frac{^1k_R(\tau_0')^{-1}[D_3O^+]}{^1k_R(\tau_0')^{-1}[D_3O^+] + \tau_0^{-1}\{^1k_{-R} + (\tau_0')^{-1}\}} \quad (2)$$

(58) It was assumed that the triplet–triplet energy transfer from triplet benzophenone to the ground state of α-RH occurred completely under the experimental conditions: [benzophenone] = $\sim 10^{-2}$ M; [α-RH] = $\sim 10^{-3}$ M at 300 K. Nanosecond ruby laser photolyses of benzophenone at 347 nm showed that the $T_n \leftarrow T_1$ absorption of benzophenone at 525 nm disappeared in the presence of α-RH ($\sim 10^{-3}$M) just after pulsing, and immediately the new absorption at 435 nm ascribed to the $T_n \leftarrow T_1$ absorption of α-RH appeared.

(59) Vogelmann, E.; Rauscher, W.; Traber, R.; Kramer, H. E. A. *Z. Phys. Chem. (Wiesbaden)* **1981**, *124*, 13.

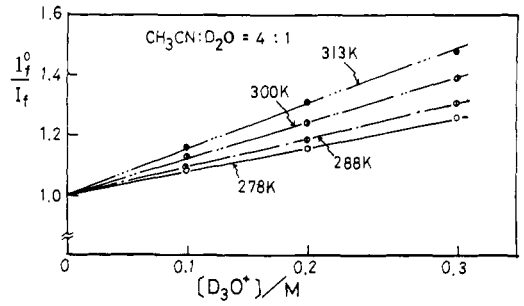

Figure 7. Temperature effects on I_f^0/I_f as a function of $[D_3O^+]$.

Table IV. Temperature Effects on ${}^1k_q$ ($\simeq {}^1k_R$) and Activation Parameters of α-RH[a]

		solvent H_2O (or D_2O): CH_3CN	${}^1k_q{}^b/10^9\ M^{-1}\ s^{-1}$ quencher H^+	quencher D^+	${}^1k_q{}^H/{}^1k_q{}^D$
T/K	278	4:1	0.88	0.43	2.0_5
		1:4	0.11	5.4×10^{-2}	2.0_4
	288	4:1	0.99	0.45	2.2
		1:4	0.12	6.5×10^{-2}	1.8_5
	300	4:1	1.0	0.51	2.1_2
		1:4	0.16	8.9×10^{-2}	1.8
	313	4:1	1.1_1	0.61	1.8_2
		1:4	0.2	0.12_7	1.6_7
$(\Delta H^{\ddagger})^*$/ kcal mol^{-1}		4:1	0.5	1.3	
		1:4	2.8	3.2	
$(\Delta S^{\ddagger})^*$/eu		4:1	-1.3_5	$-17._4$	
		1:4	−9.6	−9.6	

[a] Experimental errors within ±5%. [b] The ${}^1k_q$ values were determined from the Stern-Volmer plots and τ_0. The temperature effects on τ_0 in H_2O (or D_2O)-CH_3CN mixtures were scarcely observed within the experimental errors under the experimental conditions.

On the assumption that the value of $(\tau_0')^{-1}$ mainly consisting of the radiationless transition (internal conversion) of ${}^1(\alpha\text{-RHD})^*$ is greater than that of ${}^1k_{-R}$ for the back reaction, eq 2 can be simplified to

$$({}^1\Phi_R)^{-1} = \left(1 + \frac{{}^1k_D}{{}^1k_H}\right)\left(1 + \frac{1}{{}^1k_R\tau_0[D_3O^+]}\right) \qquad (3)$$

For instance, the plot of $({}^1\Phi_R)^{-1}$ as a function of $[D_3O^+]^{-1}$ for the D_2O–CH_3CN (4:1) system is shown in Figure 6, which gives a straight line. For the slope and intercept of the plot, the values of ${}^1k_R$ and ${}^1k_H/{}^1k_D$ were obtained to be 6.0 (±1.0) × 10^8 M^{-1} s^{-1} and 1.7 (±0.3) for the D_2O–CH_3CN (4:1) system, respectively, and 8.1 (±1.0) × 10^7 M^{-1} s^{-1} and 2.0 (±0.5) for the D_2O–CH_3CN (1:4) system, respectively, at 300 K. These ${}^1k_R$ values are very close to those (${}^1k_q$) of the proton-induced fluorescence quenching of α-RH at 300 K (Table I) within the experimental error. Therefore, eq 4 holds approximately

$${}^1k_q \simeq {}^1k_R \qquad (4)$$

This finding shows that proton-induced quenching proceeds via electrophilic protonation at one of the carbon atoms of the aromatic ring, leading to the hydrogen exchange or isotope exchange.

Temperature Effects on Isotope-Exchange Reactions in the Excited and Ground States. Temperature effects upon the H–D isotope exchange reactions both in the excited and ground states have been studied. The protonation rate constants ${}^1k_R$ in the excited state of α-RH were estimated by measurements of the ${}^1k_q$ values at the corresponding temperatures using eq 4. The plot of ${}^1k_q$ as a function of $[D_3O^+]$ gives a straight line as shown in Figure 7. From the slopes and τ_0, the ${}^1k_q$ ($\simeq {}^1k_R$) values at several temperatures can be determined. The quenching data for α-RH at several temperatures are summarized in Table IV. The activation parameters for the photochemical reaction are also listed in Table IV. We assumed that the activation parameters for ${}^1k_R$ are almost equal to those for ${}^1k_q$ on the basis of the relation in eq 4. The kinetic isotope effects ${}^1k_q{}^H/{}^1k_q{}^D$ were determined to be 1.7–2.2.

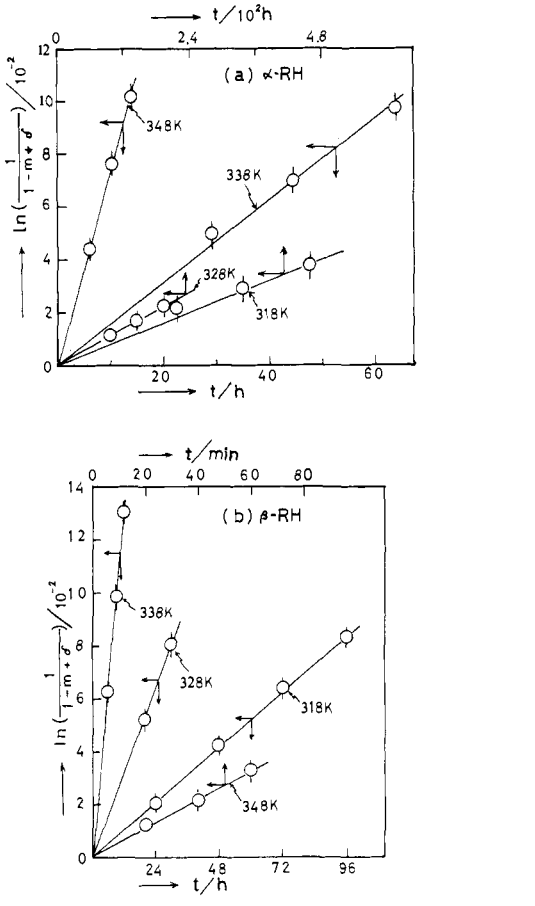

Figure 8. Plots of ln $(1 - m + \delta)^{-1}$ vs. the reaction time t for the thermal isotope-exchange reactions of α-RH (a) and β-RH (b) at several temperatures.

On the other hand, the pseudo-first-order rate constants (k') for thermal isotope-exchange reactions were measured using a 1 × 10^{-2} M RH solution (D_2O:CH_3CN = 1:4) in the presence of D_2SO_4 (0.05 M) at several temperatures (318–348 K)

$$RH + D_3O^+ \xrightarrow[\Delta]{k} RD + HD_2O^+ \qquad (5)$$

where k is the second-order rate constant and $k' = k[D_3O^+]$. The k' value is given by

$$\ln\left(\frac{1}{1 - m + \delta}\right) = k't \qquad (6)$$

where m denotes the apparent ratio for the thermal H–D isotope exchange reactions obtained from the MS parent peaks at m/e = 158 and 159 and δ is the ratio for the naturally abundant ^{13}C of RH (0.123). The plots of ln $\{1/(1 - m + \delta)\}$ vs. the reaction time t are shown in Figure 8, which agree well with eq 6. From the slopes in Figure 8, the values of k' can be determined (see Table V). As stated above, the thermal reaction rate k' for β-RH is greater than that for α-RH in contrast to the ${}^1k_q$ value in the photochemical isotope-exchange reaction. The Arrhenius plots of log k' vs. T^{-1} gave a straight line. The activation parameters obtained are listed in Table V.

Let us compare the activation parameters both for photochemical and thermal H–D isotope exchange reactions of α-RH in the D_2O–CH_3CN (1:4) system (Tables IV and V): (1) the value of the enthalpy of activation $(\Delta H^{\ddagger})^*$ for the photochemical reaction is very small compared with that for the thermal reaction, and (2) the value of the entropy of activation $(\Delta S^{\ddagger})^*$ in the excited state is more negative than that in the ground state. For α-RH the thermal reaction proceeds via a high potential barrier (27.3

Table V. Pseudo-First-Order Rate Constants k' and Activation Parameters for Thermal Isotope-Exchange Reactions of RH[a,b]

sample	k' s^{-1} 318 K	328 K	338 K	348 K	$\Delta H^{\ddagger}$/kcal mol^{-1}	$\Delta S^{\ddagger}$/eu
α-RH	$4.0_3 \times 10^{-8}$	1.6×10^{-7}	$6.9_7 \times 10^{-7}$	$2.0_6 \times 10^{-6}$	$27._3$	-6.6_7
β-RH	$2.4_3 \times 10^{-7}$	$7.3_1 \times 10^{-7}$	3.0×10^{-6}	8.9×10^{-6}	$26._4$	-6.2_7

[a] The concentration of RH was 1×10^{-2} M in a D_2O-CH_3CN (1:4) mixture with $[D_2SO_4] = 0.05$ M. [b] Experimental errors within ±5%.

Table VI. Reactive Indices for Electrophilic Reactions in the Ground and Excited States of RH[a]

reactive index	sample	state	atom (r) 1	2	3	4	5	6	7	8	reactive position (obsd)
q_r[b]	α-RH	^1A	0.9828	*1.0470*	0.9944	1.0202	1.0017	0.9978	1.0037	0.9976	2
		^1L_b	0.9577	1.0306	1.0013	0.9752	0.9968	1.0212	1.0141	0.9979	
		^1L_a	0.9789	1.0055	0.9999	0.9838	*1.0367*	1.0192	1.0041	*1.0424*	5,8
	β-RH	^1A	*1.0467*	0.9844	1.0276	0.9936	0.9989	1.0045	0.9986	1.0035	1
		^1L_b	1.0284	0.9838	1.0202	1.0120	1.0102	1.0207	0.9992	1.0030	
f_r[b]	α-RH	^1A	*0.3466*	0.2048	0.1320	0.4022	0.2968	0.1094	0.1408	0.2817	2
		^1L_b	0.0698	0.1053	0.1147	0.0665	0.0777	0.1165	0.1128	0.0789	
		^1L_a	0.1534	0.0631	0.0757	0.1461	*0.1706*	0.0823	0.0753	*0.1734*	5,8
	β-RH	^1A	*0.4190*	0.2010	0.0588	0.3100	0.3139	0.1908	0.0922	0.3504	1
S_r[b]	α-RH	^1A	0.0423	*0.0591*	0.0482	0.0490	0.0362	0.0463	0.0506	0.0344	2
		^1L_b	0.0944	0.2798	0.2876	0.0960	0.0976	0.2857	0.2844	0.0976	
		^1L_a	0.1655	0.1224	0.1282	0.1622	*0.1786*	0.1337	0.1293	*0.1803*	5,8
	β-RH	^1A	*0.0502*	0.0485	0.0533	0.0386	0.0403	0.0427	0.0491	0.0439	1
L_r^{+}[c]	α-$^+$RHD			*1.2626*	2.3439	1.0385	1.5768	2.2725	1.8719	1.9496	2
$(L_r^{+})^*$				−0.0202	0.4849	0.3002	*0.2505*	0.2318	0.1110	*0.0787*	5,8
L_r^{+}[c]	β-$^+$RHD		*1.0803*		1.7718	1.9833	1.9218	1.7344	2.2469	1.4929	1
$(L_r^{+})^*$			0.3575		0.3390	0.9199	0.2531	0.6016	0.4863	0.7930	

[a] For details see the text. [b] Calculated by a semiempirical SCF MO CI method. [c] Calculated by an extended-Hückel MO method. The total energies of α- and β-RH were −1098.5225 and −1098.3359 eV, respectively.

kcal/mol), whereas the photochemical reaction only needs a small one (3.2 kcal/mol). The negative values of $\Delta S^{\ddagger}$ may result from changes in solvation (hydration) providing the marked contribution to entropy changes especially for the photochemical reaction. The reactive state is the lowest excited singlet state of α-RH (^1L_a) having a CT character produced by reorientation of solvent molecules, as described above. If we keep it in mind, the large negative value of $(\Delta S^{\ddagger})^*$ in the excited state can be well understood. For the thermal reactions (the reactive positions: 2 for α-RH; 1 for β-RH), for β-RH the $\Delta H^{\ddagger}$ value is slightly less than that for α-RH and the $\Delta S^{\ddagger}$ value is also slightly less negative. A similar tendency has been reported in the thermal and photochemical exchange reactions of naphthalene at high concentrations of sulfuric acids, studied by Stevens and Strickler[26,60] and also in the thermal detritiation of 1 and 2-naphthalene-t_1 in anhydrous trifluoroacetic acid by Eaborn and Taylor.[61]

Theoretical Considerations. Theoretical MO calculations based on quantum mechanical methods may give us much information for chemical reactions. The reactive indices for the electrophilic reactions both in the ground and excited states have been calculated by means of semiempirical SCF MO CI and extended-Hückel MO methods. The calculated reactive indices (q_r: charge density;[36] f_r: frontier electron density;[38a] S_r: super delocalizability;[38b] and L_r: the localization energy)[39] are summarized in Table VI. The reactive positions in α- and β-RH in Table VI show that they are completely different from each other. This is due to the difference in electronic structures not only between α- and β-isomers but also between the excited and ground states. The reactivity for electrophilic protonation (or deuteration) at the proper carbon atoms of RH can be explained from the corresponding formal charge (or charge density). The formal charges at the proper carbon atoms are −0.0367 and −0.0424 at positions 5 and 8 of the excited α-RH (^1L_a), respectively; −0.0017 and +0.0024 at positions 5 and 8 of the ground α-RH; −0.0470 and −0.0055 at position 2 of ground and excited states of α-RH; −0.407 and −0.0284 at position 1 of ground and excited states of β-RH. The exchange positions of RH entirely agree with the positions having a negatively large formal charge (or large charge density) both in the ground and excited states. These facts show that the photochemical and thermal isotope-exchange reactions proceed via electrophilic reactions. For the isotope exchange in the excited state of α-RH, the reactivity of carbon atom 8 with D^+ is not so high compared with that of carbon atom 5 as expected from the corresponding formal charge. This may be mainly due to steric hindrance by the methoxy substituent (peri-effect). Similar features were obtained in the reactive indices f_r and S_r for the electrophilic reactions, although the prediction of the reactive positions by S_r was superior to that by f_r.

It is of interest to compare the relation between the electronic structure in the excited state of other compounds and the value of ^1k_q ($\simeq {}^1k_R$). For example, in the excited state of 1-aminopyrene charge migration from the amino group to the pyrene ring, i.e., the intramolecular charge transfer, may take place in polar media as well as those in naphthylamines,[15] 1-naphthol,[19] and α-RH. The formal charges at the proper nitrogen atom of 1-aminopyrene calculated by a semiempirical SCF MO CI method are 0.209 and 0.340 in the ground and excited states, respectively.[16] However, the charge density at the proper carbon atom of the pyrene ring is not so large (<1.073) since the migrated charge is widely distributed on the carbon atoms of the pyrene ring. The electrophilic interaction between H^+ (or D^+) and the proper carbon atom in the aromatic ring is locally restricted as described above. As a result, the value of ^1k_q for 1-aminopyrene becomes small in comparison with those of naphthylamines (see Table I). Similar behavior in the case of phenanthrylamines has been shown.[18]

The localization energies L_r^{+} calculated by an extended-Hückel MO method were almost consistent with the reactive positions for the thermal isotope-exchange reactions of RH. The L_r^{+} values in the ground state (1.263 eV for α-RH at position 2 and 1.080 eV for β-RH at position 1) are approximately equal to those (1.18_4 and 1.14_5 eV, respectively) of the enthalpies of activation $\Delta H^{\ddagger}$ obtained experimentally in the thermal reactions (see Table V). The localization energies $(L_r^{+})^*$ in the excited state were estimated from the equation

$$(L_r^{+})^* = L_r^{+} + \Delta E_\sigma^* - \Delta E_{RH}^* \quad (7)$$

where ΔE_σ^* denotes the transition energy in the corresponding

(60) Stevens, C. G.; Strickler, S. J. *J. Am. Chem. Soc.* **1973**, *95*, 3918.
(61) Eaborn, C.; Taylor, R. *J. Chem. Soc.* **1961**, 247.

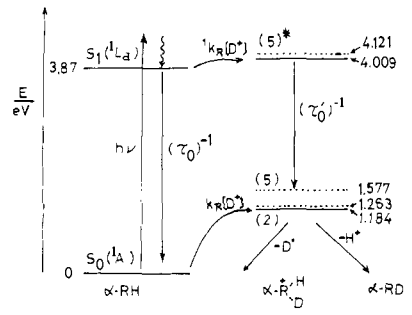

Figure 9. A potential energy state diagram for photochemical and thermal isotope-exchange reactions of α-RH. There are three types of σ complexes: (5)*, (5), and (2), where (5)* denotes the excited state of the σ complex deuterated at position 5 of the naphthalene ring in the S_1 (^1L_a) state of α-RH, (5) is the ground σ complex produced from the radiationless transition $(\tau_0')^{-1}$ of (5)*, (2) is the ground σ complex deuterated at position 2 of the naphthalene ring in the ground state of α-RH, and ^1k_R and k_R ($\simeq 1.5\ k$) are the corresponding deuteration rate constants in the excited and ground states, respectively. Their energy levels were determined experimentally (full line) and theoretically (dotted line); for details, see the text.

σ-complex calculated by an extended-Hückel MO method and ΔE_{RH}* the 0–0 transition energy S_1–S_0 (3.87 eV for S_1-(^1L_a)–$S_0(^1A)$ in α-RH; 3.68 eV for $S_1(^1L_b)$–$S_0(^1A)$ in β-RH) obtained experimentally. However, it was unsuitable for the excited state to predict the reactive positions of α-RH from the $(L_r^{\ddagger})$* values. The reason for the discrepancy may be that the localization energy calculated by means of an extended-Hückel MO method is a nice approximation for the ground σ complex but not good for the excited one; probably, the transition energy ΔE_σ* is not so accurate. The energy levels $(E_\sigma^*)_{calcd}$ and $(E_\sigma)_{calcd}$ for the excited and ground states of α-$^+$RHD (deuterated at position 5) were estimated to be 4.121 and 1.577 eV, respectively, from the extended-Hückel MO method. The energy level of the excited α-$^+$RHD lies slightly above that (3.87 eV) of the relaxed fluorescent state (^1L_a) by $(L_r^{\ddagger})^* \simeq 0.25$ eV as shown in Figure 9. The enthalpy of activation $(\Delta H^{\ddagger})^*$ (0.139 eV) for deuteration at position 5 in the excited state of α-RH obtained experimentally accords approximately with the calculated value of $(L_r^{\ddagger})^*$. The energy level of E_σ* in (α-RHD)* is, therefore, experimentally derived from the equation

$$(E_\sigma^*)_{exptl} = \Delta E_{RH}^* + (\Delta H^{\ddagger})^* = 4.009 \text{ eV} \qquad (8)$$

The value of $(E_\sigma^*)_{exptl}$ is very close to the energy level in the excited σ* complex [$(E_\sigma^*)_{calcd}$ = 4.121 eV] obtained theoretically. Thus, the σ complex produced by the electrophilic reaction at position 5 of (α-RH)* (^1L_a) is probably in the electronically excited state (5)*. The decay rate from (5)* to the ground state (5), i.e., internal conversion, is believed to be very much faster than those of other competitive processes. The detection of the intermediate of the σ-complex has been attempted by means of nanosecond Nd^{3+}: YAG laser spectroscopy at 266 nm.[62] However, its detection has not yet been successful. Both the $T_n \leftarrow T_1$ absorption (λ_{max} = 430 nm) of α-RH and the absorption of its cation radical (λ_{max} = 680 nm)[63] were observed, and immediately after pulsing they were quenched by protons indicating that the quenching by protons occurred effectively in the excited singlet state.[62] Further study for detection of the σ complex will be needed in near future. Electrophilic deuteration in the excited or ground state of α-RH can be explained by an energy state diagram as shown in Figure 9. After the formation of (5) via (5)* deuterated at position 5 in the excited state (^1L_a) or that of (2) deuterated at position 2 in the ground state (^1A) of α-RH, H^+, or D^+ dissociation with the rate constants ^1k_H and ^1k_D (see Scheme I) may occur to yield the isotope-exchange product or the starting material, respectively, whose isotope effect ($^1k_H/^1k_D$) on the dissociation process is found to be about 2 in the D_2O–CH_3CN (1:4) system at 300 K. The real value of the rate constant k_R for deuteration in the ground state of α-RH can be estimated to be about 1.5 times greater than that of k (see eq 5) in D_2O–CH_3CN (1:4) at 300 K.

Ionic reactions may be discussed from the hard and soft acids and bases (HSAB) concept,[64,65] as has been theoretically studied by Klopman:[66] that is, the total perturbation energy consists of the Coulombic (charge-controlled) and covalent (frontier-controlled) terms. The charge density of the proper carbon atom of the aromatic ring of α-RH increases upon excitation, resulting in an increase of the Coulombic perturbation energy between the proper carbon atom and H^+ (or D^+). The excited species is regarded as a soft base since the potential energy difference between the energy levels of HOMO in the excited α-RH and LUMO in hydronium ion (+0.42 eV)[66] is estimated to be less than 1 eV. As a result, the covalent term which correlates with the super delocalizability S_r also increases upon excitation. In other words, the basicity of the proper carbon atom of the aromatic ring of α-RH increases markedly in the excited state compared to that in the ground state. This is the reason why the reactivity of isotope exchange in the excited state is much greater than that in the ground state. Strictly speaking, it is impossible to compare directly the rate constants for electrophilic attack at the same reactive position both in the excited and ground states of α-RH, since the reactive positions are different from each other (mainly position 5 for the excited state and position 2 for the ground state). However, if we compare only the values for both states, the value of the deuteration rate constant ($^1k_R \simeq 1.1_5 \times 10^8\ M^{-1}\ s^{-1}$) in the excited state estimated from ^1k_q at 318 K is very much greater than that in the ground state ($k_R \simeq 6.0 \times 10^{-7}\ M^{-1}\ s^{-1}$ estimated from $k = 4.0 \times 10^{-7}\ M^{-1}\ s^{-1}$ at 318 K on the assumption that the value (k_H/k_D) of isotope effect on deprotonation from the σ complex (2) is equal to 2.

Finally, the isotope-exchange reactions both in the excited and ground states can be understood by taking account of the reactive indices for electrophilic reactions calculated by the usual MO methods.

Summary

(1) Proton-induced quenching of α-RH proceeds via electrophilic protonation at the proper carbon atom of the aromatic ring in the lowest excited singlet state (^1L_a) in polar media, leading to hydrogen exchange or isotope exchange mainly at position 5 (slightly at position 8) of the naphthalene ring. It was found that the rate constant ^1k_R for electrophilic protonation to the carbon atom of the aromatic ring in the excited state is almost equal to that of ^1k_q for proton-induced quenching. An intramolecular CT structure in the excited state is responsible for the proton-induced quenching. The isotope-exchange reaction via the triplet state of α-RH was negligibly small (about 5% compared with that via the excited singlet state).

(2) For β-RH, both proton-induced fluorescence quenching and isotope exchange in the excited state (^1L_b) scarcely occurred at moderate acid concentrations at 300 K.

(3) At higher temperatures (≥318 K), the thermal isotope-exchange reactions of α- and β-RH took place at positions 2 and 1, respectively; the exchange rate for the latter was faster than that for the former, contrary to that of photochemical reactions.

(4) The H–D isotope exchange reactions in both the excited and ground states of RH can be elucidated by taking account of the reactive indices derived from the usual MO calculations (semiempirical SCF MO CI and extended-Hückel MO methods) indicating that both photochemical and thermal isotope-exchange reactions proceed via electrophiic attack at the proper carbon atoms in the excited and ground states of the aromatic ring of α-RH.

(62) T. Kobayashi, unpublished results.
(63) The assignment for the intermediate at 680 nm was indebted to Professor T. Shida of Kyoto University.
(64) Pearson, R. G. "Hard and Soft Acids and Bases"; Dowden, Hutchinson, and Ross: Philadelphia, 1973.
(65) Ho, T.-L, "Hard and Soft Acids and Bases Principle in Organic Chemistry"; Academic Press: New York, 1977.
(66) Klopman, G. *J. Am. Chem. Soc.* **1968**, *90*, 223.

(5) The value of the enthalpy of activation $(\Delta H^{\ddagger})^*$ in the photochemical reaction is very small compared with that $(\Delta H^{\ddagger})$ in the thermal reaction. For the entropy of activation, the value $(\Delta S^{\ddagger})^*$ in the former is more negative than that $(\Delta S^{\ddagger})$ in the latter. On the basis of experimental results, the isotope-exchange mechanism of α-RH can be accounted for by a potential energy state diagram with the aid of an extended-Hückel MO method as shown in Figure 9. The electrophilic deuteration of α-RH in the excited or ground state may produce the excited (**5**)* or ground (**2**) σ complex, respectively. After the formation of the ground σ complex (**5**) from the decay of the excited one (**5**)* for the photochemical reaction or the ground σ complex (**2**) for the thermal reaction, deprotonation or deuteration from the complexes gives the isotope-exchange product or the starting material, respectively.

(6) The kinetic isotope effects ${}^1k_q^H/{}^1k_q^D$ ($\simeq {}^1k_R^H/{}^1k_R^D$) and ${}^1k_H/{}^1k_D$ in α-RH were determined to be 1.7-2.2 and 1.7-2.0, respectively.

Registry No. 1-Methoxynaphthalene, 2216-69-5; 2-methoxynaphthalene, 93-04-9; 1-cyanonaphthalene, 86-53-3; 2-cyanonaphthalene, 613-46-7; naphthalene, 91-20-3; pyrene, 129-00-0.

Nitrogen Quadrupole Coupling Measurements on ON-NO_2 Using the Flygare-Balle Pulsed-Beam Spectrometer

Stephen G. Kukolich*

Contribution from the Noyes Chemical Laboratory, University of Illinois, Urbana, Illinois 61801.
Received May 3, 1982

Abstract: High-resolution measurements of the $1_{01} \leftarrow 0_{00}$, $2_{12} \leftarrow 1_{11}$, $2_{02} \leftarrow 1_{01}$, $2_{11} \leftarrow 1_0$, $3_{12} \leftarrow 3_{13}$, and $4_{13} \leftarrow 4_{14}$ transitions in the ON-NO_2 complex were made by using a pulsed-beam, Fourier transform microwave spectrometer. Nearly all hyperfine structure components were resolved on observed transitions except for the $2_{02} \leftarrow 1_{01}$ group. The quadrupole coupling tensors in the principal axis system were determined for both nitrogen atoms. The nitrogen quadrupole coupling components for the NO group are $eQq_{aa} = -1.7766 \pm 0.0037$ MHz and $eQq_{bb} = 0.0585 \pm 0.0021$ MHz. For the NO_2 group $eQq_{aa} = -0.5260 \pm 0.0035$ MHz and $eQq_{bb} = -4.1941 \pm 0.0018$ MHz. The rotational constants obtained are $A = 12412 \pm 22$ MHz, $B = 4226.530 \pm 0.012$ MHz, and $C = 3152.966 \pm 0.012$ MHz. Rotational transition frequencies and estimates of spin-rotation interaction strengths are given. The observed quadrupole coupling strengths are substantially different from those observed for the free NO and NO_2 molecules.

Introduction

The ON-NO_2 complex is a ${}^1\Sigma$ diamagnetic complex formed from the two paramagnetic molecules NO and NO_2. The structure of this complex was determined by Brittain et al.[1] from a detailed microwave study involving seven isotopic species. Although the structure appears to have been accurately determined, the resolution was not high enough for an accurate determination of the quadrupole coupling. The two inequivalent, spin-1 nitrogen atoms in this molecule cause rather complex hyperfine structure patterns for most of the observed rotational transitions. This study was undertaken to obtain the quadrupole coupling tensor components at both nitrogen sites in this molecule. The quadrupole coupling components may be used to obtain the electric field gradients and can be used to determine electronic structure and bonding parameters for the N-N bond. There are many examples of inorganic complexes involving the nitrosyl group, and this case may be helpful in characterizing the bonding in this group of complexes.

Experimental Section

The microwave spectra were observed by using a pulsed-beam, Fourier transform spectrometer developed by Balle, Flygare, and co-workers.[2,3] A mixture of 2% NO and 2% NO_2 in argon at 1-2 atm was rapidly expanded into the region between two spherical mirrors by using a pulsed solenoid valve operating at about 1 pulse/s. A 90° microwave pulse of 2-μs duration was used to excite a "free induction decay" signal from the gas sample between the mirrors. The "free induction decay" signal was beat down to 30 MHz by using a superhet receiver and then beat against a 30-MHz signal in a balanced mixer. The resulting beat signal was digitized at 0.5 μs/point for 256 points. The digitized signals are averaged and Fourier transformed to obtain the frequency spectrum with a resolution of 3.9 kHz/point. The beam is directed perpendicular to the cylinderical axis of the cavity to minimize Doppler broadening. Some Doppler broadening or splitting is observed due to the finite divergence angle of the molecular beam. The effective resolution is 12 kHz for typical measurements. The gasses were typically 95% pure or better and obtained from commercial suppliers. Signals could also be observed by mixing a 1:4 mixture of oxygen and nitric oxide in argon to form the ON-NO_2.

Table I. Center Frequencies for Rotational Transitions Observed in ON-NO_2

transition	frequency, MHz	transition	frequency, MHz
$1_{01} \leftarrow 0_{00}$	7379.541 (12)	$2_{11} \leftarrow 1_{10}$	15832.551 (12)
$2_{12} \leftarrow 1_{11}$	13685.411 (12)	$3_{12} \leftarrow 3_{13}$	6435.669 (12)
$2_{02} \leftarrow 1_{01}$	14660.6 (1)	$4_{13} \leftarrow 4_{14}$	10695.832 (12)

Results and Data Analysis

Four R-branch ($\Delta J = +1$) and two Q-branch ($\Delta J = 0$) were measured in the present work. The center frequencies of the observed transitions are listed in Table I. An attempt was made to observe the $6_{24} \leftarrow 6_{25}$ transition near 5964 MHz and the $7_{25} \leftarrow 7_{26}$ transition near 9876 MHz, but neither of these transitions was observed. The rapid expansion of the beam produces very effective rotational cooling of the gas mixture, and it is believed that these higher J transitions were not sufficiently well populated.

The simplest observed transition was the $1_{01} \leftarrow 0_{00}$ at 7379.54 MHz. Only the $J = 1$ level is split by the nitrogen quadrupole

* Permanent address: Department of Chemistry, University of Arizona, Tucson, AZ 85721.

(1) A. H. Brittain, A. P. Cox, and R. L. Kuczkowski, *Trans. Faraday Soc.*, **65**, 1963-1974 (1969).
(2) T. J. Balle and W. H. Flygare, *Rev. Sci. Instrum.*, **52**, 33-45 (1981).
(3) T. J. Balle, E. J. Campbell, M. R. Keenan, and W. H. Flygare, *J. Chem. Phys.*, **72**, 922-932 (1980); **71**, 2723-2724 (1979).

0002-7863/82/1504-6927$01.25/0